Vol. 44 — N° 3 09 20 P. 537 – 551

GEOSTANDARDS and GEOANALYTICAL RESEARCH

Nitrogen Mass Fraction and Stable Isotope Ratios for Fourteen Geological Reference Materials: Evaluating the Applicability of Elemental Analyser Versus Sealed Tube Combustion Methods

Toby J. **Boocock** (1)*, Sami **Mikhail** (1), Julie **Prytulak** (2), Tommaso **Di Rocco** (1, 3) and Eva E. **Stüeken** (1)

(1) School of Earth and Environmental Sciences, University of St Andrews, St Andrews, KY16 9AL, UK
(2) School of Earth Sciences, University of Durham, Durham, DH1 3LE, UK
(3) Isotope Geology Department, Georg-August-Universität Göttingen, Göttingen, 37077, Germany
* Corresponding author. e-mail: tjb7@st-andrews.ac.uk

Thirteen commercially available silicate reference materials (RM) and one in-house reference material, eleven of which have no previously published values, were analysed for nitrogen mass fraction and isotopic ratios with an Elemental Analyser (EA), and a Sealed Tube Combustion line, coupled to a continuous flow isotope ratio mass spectrometer (IRMS). These materials ranged from < 10 μg g^{-1} to 1% *m/m* nitrogen mass fractions and $\delta^{15}N$ of -0.5 to +19.8‰. Existing nitrogen RM BHVO-2, MS.5 and SGR-1b were used to assess the accuracy of the data from the sealed tube combustion line, which was found to be in good agreement with existing published values. In contrast, the EA-IRMS failed to fully liberate nitrogen from all silicate rocks and minerals (achieving a mean of 44 ± 10% nitrogen yield) resulting in kinetic fractionation of isotope values by -1.4‰ on average. Therefore, sealed tube combustion is better suited for analyses of silicate-bound nitrogen. The EA worked reliably for organic samples, but care should be taken when using the EA for silicate nitrogen research. Moving forward, it is recommended that BHVO-2, Biotite-Fe, FK-N and UB-N be used as quality control materials as they appear to be most reproducible in terms of nitrogen mass fraction (relative error < 10%, 1*s*), and isotopic composition (< 0.6‰, 1*s*).

Keywords: nitrogen, reference materials, stable isotopes, method validation, geochemistry.

Received 21 Jan 20 – Accepted 19 May 20

Nitrogen (N) is the seventh most abundant element in the solar system, it makes up 78% of the modern atmosphere, and it is an essential element for life. Previously considered solely as an *atmophile* element (Goldschmidt 1926), it has become increasingly apparent that a significant proportion of terrestrial N is contained within the solid Earth (e.g., Li *et al.* 2013). Several experimental and theoretical studies have revealed that N is compatible with numerous silicate phases across a large range of geochemical conditions (e.g., N^{3-}, NH_2^-, N_2, NH_4^+; Busigny and Bebout 2013, Li *et al.* 2013, Mikhail and Sverjensky 2014, Yoshioka *et al.* 2018). These observations raise questions about how N is cycled through the Earth's crust and mantle, and how the geological N cycle has evolved over geological time. Addressing these fundamental questions requires refined analytical methods to permit precise and accurate elemental and isotopic determinations of trace abundances of nitrogen (μg g^{-1}) in silicate phases with high melting temperatures. Furthermore, matrix-matched silicate reference materials (RM) are required to evaluate data quality between laboratories.

At present, published nitrogen isotopic data for silicate RM other than sediments (such as SGR-1b, Dennen *et al.* 2006) are limited to USGS BHVO-2 (Feng *et al.* 2018) and a few internal, not commercially available, laboratory RM such as MS#5 Mica Schist (Busigny *et al.* 2005, Feng *et al.* 2018) and WE-2 Fuchsite (Bebout and Sadofsky 2004). As interest in the nitrogen cycle in silicate systems increases, the need for representative and commercially available RM becomes paramount. Here and elsewhere, stable N isotopes are expressed in delta notation relative to atmospheric N_2 gas

doi: 10.1111/ggr.12345

$$\delta^{15}N = [(^{15}N/^{14}N)_{sample}/(^{15}N/^{14}N)_{air} - 1] \quad (1)$$

Several methods can be applied for the extraction and quantification of nitrogen abundances and isotopic values from geological materials. For example, if the target is a fluid or gaseous inclusion, then online vacuum-crushing systems are applicable (adopting the methodology of noble gas geochemistry – Marty *et al.* 1995, Barry *et al.* 2012). However, this approach does not liberate lattice-bound nitrogen from silicate phases, which requires destruction of mineral lattices. This is commonly achieved by some style of high vacuum combustion system such as flash combustion in an elemental analyser (EA) or by long-duration online diffusion and/or stepped combustion (e.g., Busigny *et al.* 2005, Mikhail *et al.* 2014).

The sealed tube combustion method builds upon gas-line mass spectrometry and gas separation and purification techniques developed by the likes of Urey (1947) and Craig (1953). The method was initially developed for the combined analysis of both $^{15}N/^{14}N$ and $^{13}C/^{12}C$ (e.g., Stuermer *et al.* 1978, Minagawa and Wada 1986) in organic (kerogen)-rich sediments but has since been modified for the analysis of N in inorganic silicate samples (Bebout and Fogel 1992, Busigny *et al.* 2005, Ader *et al.* 2006, Bebout *et al.* 2007, Feng *et al.* 2018). This method has been shown to provide accurate results for lattice-bound nitrogen in silicate bulk rock and mineral phases (Boyd and Pillinger 1990, Bebout and Fogel 1992, Boyd *et al.* 1994, Bebout and Sadofsky 2004, Busigny *et al.* 2005, Ader *et al.* 2006, Feng *et al.* 2018). Fundamentally, the method works by combining high-temperature combustion (*ca.* 900–1000 °C) with long-term diffusion of N from the lattice structure (held at temperature for 6 h), which results in total liberation of lattice-bound nitrogen species (Busigny *et al.* 2005, Bebout *et al.* 2007). However, sealed tube combustion is relatively expensive and labour-intensive when compared with flash combustion.

Flash combustion has the advantage of being relatively cheap, fast and automated. This technique is commercially available and packaged as appliances known as EA. Flash combustion applies one combustion step (*ca.* 1600 °C) over a few seconds. The resulting gas is then transferred to an isotope ratio mass spectrometer (IRMS) via a water trap and a gas chromatograph column. This technique is presently used for determining stable isotopic ratios (C, N, S) of a range of geological samples (e.g., Kubota 2009, Stüeken *et al.* 2015). However, previous studies have questioned the efficiency of the EA method for releasing lattice-bound nitrogen from bulk rock silicate samples (Bräuer and Hahne 2005, Ader *et al.* 2006, Johnson *et al.* 2017, Feng *et al.* 2018). Building upon that work, we present a systematic comparison of the sealed tube and flash combustion methods for different silicate matrices represented by the fourteen RM to assess the validity of flash combustion versus sealed tube combustion.

Materials

Existing N RM Mica Schist MS#5 (Busigny *et al.* 2005), Basalt BHVO-2 (Wilson 1997) and Shale SGR-1b (Dennen *et al.* 2006) were used to assess the quality of the new sealed tube combustion method. MS#5 is an in-house rock reference material from the Institute du Physique du Globe de Paris. It is a garnet-bearing mica schist from the Moine Supergroup of Scotland composed of quartz, plagioclase, garnet, white mica and biotite (Busigny *et al.* 2005). Approximately 60 g of MS#5 was crushed and homogenised at IPGP (< 160 μm). BHVO-2 is a sample of Hawaiian basalt sourced from the Halemaumau crater, collected and prepared by the USGS, and now a well-established isotopic reference material for a large number of isotope systems (e.g., $\delta^{7}Li$, $\delta^{15}N$, $\delta^{26}Mg$, $\delta^{34}S$, $\delta^{51}V$; Jochum *et al.* 2005). SGR-1b is an oil-bearing shale from the Eocene Green River Formation (Dennen *et al.* 2006). In addition to these existing nitrogen RM, a number of new RM were chosen from CRPG including feldspars (Albite AL-I, Anorthosite AN-G, Felspath FK-N), micas (Biotite-Fe, Phlogopite-Mg) and serpentine (Serpentine UB-N) alongside several powdered rocks (CRPG; Granite MAN, Trachyte ISH-G, Trachyte MDO-G, USGS; Granite G3, Mica Schist SDC-1; Table 1). These cover a large range of mineral and rock matrix types and are useful for application to igneous and/or metamorphic studies.

Reagents for both the EA and for the sealed tube combustion methods were chromium oxide (part B1099, Elemental Microanalysis), silvered cobaltous cobaltic oxide (part IR1200.025, Elemental Microanalysis), quartz wool (part B1102, Elemental Microanalysis), vanadium pentoxide (part B4001, Elemental Microanalysis), copper oxide wire (4 × 0.5 mm B1125 Copper Oxide Fine Wires, Elemental Microanalysis) and copper wire (4 × 0.5 mm Copper Reduction Reagent, OEA Laboratories).

The copper oxide wire for the sealed tube method was cleaned by combustion at 950 °C in a ceramic crucible for 24 h in air. Copper wire for the sealed tube method was cleaned at 950 °C for 24 h in helium, using the furnace of the EA. Quartz tubing (6 mm ID, 9.5 mm OD; compatible with 3/8″ (9.525 mm) Swagelok ultra-torr fittings) was purchased from Technical Glass Products. All tubes were

Table 1.
List of reference materials obtained and analysed in this study, most of which do not have any existing data for nitrogen contents or isotope values

Reference Material	Lithology	Provider	Published N data?	Key references
AL-I	Albite	CRPG-CNRS	No	
AN-G	Anorthosite	CRPG-CNRS	No	
FK-N	Potash feldspar	CRPG-CNRS	No	
Mica-Fe	Biotite	CRPG-CNRS	No	
Mica-Mg	Phlogopite	CRPG-CNRS	No	
UB-N	Serpentine	CRPG-CNRS	No	
BHVO-2	Basalt	USGS	Yes	Feng *et al.* (2018)
ISH-G	Trachyte	CRPG-CNRS	No	
MDO-G	Trachyte	CRPG-CNRS	No	
MA-N	Granite	CRPG-CNRS	No	
G3	Granite	USGS	No	
SDC-1	Mica schist	USGS	No	
SGR-1b	Shale	USGS	Yes	Dennen *et al.* (2006), Stüeken *et al.* (2015)
MS#5	Mica schist	IPGP	Yes	Busigny *et al.* (2005)

Note that MS#5 is an in-house reference material at IPGP and not available commercially. CRPG = Centre de Recherches Pétrographiques et Géochemiques, CNRS = Centre National de la Recherche Scientifique, IPGP = Institut de Physique du Globe de Paris, USGS = United States Geological Survey.

cleaned of potential surficial contamination by pre-combustion at 1000 °C in air for approximately 10 h. Apart from the quartz tubing that is used to hold the samples, the vacuum line is entirely built out of stainless-steel tubing and needle valves commercially available from Swagelok and remains under vacuum at all times.

Methods

Sealed tube combustion

The sealed tube combustion system (Figure 1) was built in-house in the St Andrews Stable Isotope Geochemistry (STAiG) laboratory, following published protocols (Kendall and Grim 1990, Busigny *et al.* 2005, Bebout *et al.* 2007, Stüeken *et al.* 2015, Feng *et al.* 2018). It is composed of three parts: (a) an offline vacuum line where quartz tubes containing sample powder are evacuated and sealed; (b) a muffle furnace where the sealed tubes are heated to 950 °C to diffusively release lattice-bound N whilst converting all species to N_2 gas and (c) an online continuous flow tube cracker system where the sealed tubes are cracked within a helium carrier gas to transfer the N_2 gas to the IRMS.

Sample preparation involves cutting quartz glass tubes to lengths of 30 cm and sealing one end using an oxy-acetylene blowtorch. This tube length provides a large internal volume and thus reduces the likelihood of gas overpressure leading to tube rupture during combustion. Between 1.0 and 1.1 g of copper oxide wire were added to each tube, using a glass funnel. For the shale reference material SGR-1b, 0.5–0.55 g of copper wire was added in addition to the copper oxide because omission of copper resulted in residual nitric oxide (NO), expressed as a peak with $m/z = 30$. We postulate that this is a result of insufficient Cu in the CuO alone. CuO decomposes to produce Cu^0 and O_2 gas at high temperature; that is, the equilibrium of the reaction $2CuO = 2Cu + O_2$ shifts to the right. After the O_2 has reacted with the sample, the residual Cu reacts with any NO gas resulting in the formation of $CuO + 0.5N_2$. Below saturation, the products are $Cu + CuO + N_2$. The presence of an NO ($m/z = 30$) peak thus indicates a Cu deficiency, perhaps because it was inactivated by recalcitrant hydrocarbons present in this oil shale. Monitoring the signal at $m/z = 30$ is thus a useful way of determining if samples have undergone complete conversion. Furthermore, $m/z = 30$ allows tracking the presence of carbon monoxide (CO), which can act as an isobaric interference of N_2 isotopes. For all other silicate materials and for the caffeine and glutamic acid RM, the nitric oxide peak was absent, suggesting complete conversion of lattice-bound N to N_2. SGR-1b is the only sample to present this $m/z = 30$ peak and the only sample with significant hydrocarbon contents.

After the addition of CuO and Cu to the quartz tube, dry sample powder (typically around 0.2–0.5 g) was added with a thistle funnel to ensure that the powder reached the base of the tube. Sample powder must be prevented from sticking to the upper section of the tubes, as this section is not retained after blowtorching the tube off the vacuum line. The mass of each sample used is optimised to obtain a peak area significantly resolvable above the background of the mass spectrometer (e.g., exceeding a 10:1 signal:blank ratio) whilst also minimising the need for large amounts of sample material. Therefore, the mass of sample required is scaled based on background levels, blank size and amount of nitrogen in the sample. The masses used in this study for each RM are presented in the supplementary data tables. For samples with high N mass fractions (e.g., SGR-1b) that required small amounts of sample (0.05–1.0 mg), small capsules of quartz glass (3 mm ID, 5 mm OD, sealed on one end) were made to carry the sample powder to the base of the tube. Capsules were weighed on a microbalance and then dropped into the larger tube. The bespoke quartz capsules were preferred over silver capsules because they do not contribute (measurably) to the nitrogen blank

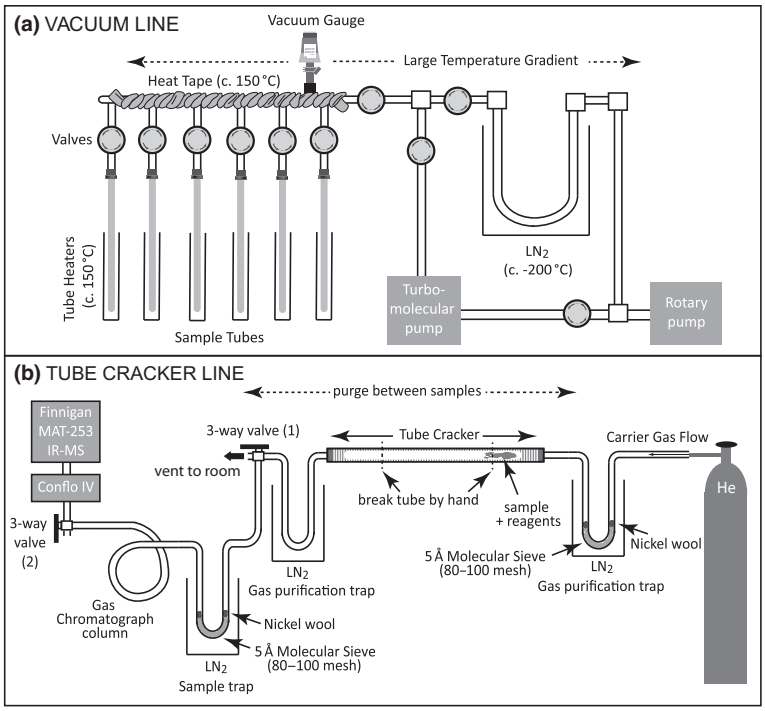

Figure 1. Schematic of (a) the offline vacuum line and (b) online tube cracker line used for the preparation and analysis of sealed tubes. (a) Samples are attached in tubes to the vacuum line for 24 h where they are pre-heated to above the boiling point of water and evacuated to 10^{-5} mbar or better. (b) After heating in a muffle furnace, sample tubes are loaded into the tube cracker under Helium carrier gas flow. Once the line is purged of air, as determined by measuring intensities of *m*/*z* = 28 and 29 on the mass spectrometer, sample tubes may be manually cracked by hand, entraining the sample gas in the helium flow. All traps are under LN_2 throughout this stage. Sample gas is left to adsorb onto the molecular sieve in sample trap for 12 min, then sample trap is thawed with +60 °C water, sending the sample gas through to the mass spectrometer.

(see Analytical blanks section, below). In addition, several other components of the set-up have the potential to contribute to the blank, including incomplete removal of air by the vacuum line, small leaks in the tube cracker line and N released from different reagents. These were continually monitored through replicate measurements of the total analytical blank (e.g., combined vacuum, reagent and tuber cracker line blank).

The packed quartz tubes were attached to the vacuum line (Figure 1) and heated to 120 °C with a tube furnace until the vacuum reached < 10^{-5} mbar. After approximately 24 h, the tubes were sealed with an oxy-acetylene blow-torch about 3–5 cm below the top and placed into the muffle furnace at 950 °C for 4 h. The furnace was then cooled to 600 °C, kept at this temperature for 2 h to allow NO to react with Cu and then cooled slowly to room temperature. The cooled tubes were then scored with a knife a few centimetres from either end and placed into the online tube cracker (Figure 1). Between samples, the line was purged with a continual helium flow to reduce the background. The helium was purified upstream of the tube cracker with a liquid nitrogen trap, filled with molecular sieve 5 Å (80–100 mesh). Downstream of the tube cracker we installed an empty liquid nitrogen U-trap to trap H_2O and CO_2 gases and potential hydrocarbons liberated from samples (Figure 1). Some previous studies have added calcium oxide (CaO) to the tubes to capture H_2O and CO_2 gases liberated from samples (Kendall and Grim 1990); however, CaO has been proven to add significantly to the analytical blank for nitrogen (Busigny *et al.* 2005). No CaO was used in this study due to the use of traps and to reduce the overall blank. The H_2O/CO_2 trap is followed by a second molecular sieve trap (5Å, 80–100 mesh) held at liquid nitrogen temperature (-190 to -210 °C), which trapped N_2 gas liberated from the sample for the purpose of cryo-focusing.

After insertion of a sealed tube into the tube cracker, the line was purged for 3 min before the scored tube was

cracked manually on both ends and the N_2 gas was released downstream to the molecular sieve nitrogen trap. The addition of a valve (three-way valve 1; Figure 1) immediately following the tube cracker apparatus reduces the internal volume of the line that requires purging of atmospheric N_2 between samples. Practically, this means that a greater number of samples (16–20 tubes including samples, RMs and blanks) can be run each day as inter-sample purging times were reduced from approximately 45 min to < 3 min. Nitrogen (N_2) gas was collected in the sample trap for 12 min before thawing with warm water placed around the outside of the trap (around +50–60 °C) to liberate the N_2 gas in a single pulse at a helium flow of 50 ml min^{-1}. Prior to entering the mass spectrometer source, the N_2 gas is further purified using a 1-m molecular sieve 5 Å packed GC column (1/8″ OD, 80–100 mesh) held at room temperature to ensure complete separation of N_2 from any potential traces of CO. We did not detect any CO peaks, suggesting complete purification of gasses. The GC column was baked out overnight with a heating tape set to around 150 °C under a helium flow of a few ml min^{-1}.

Elemental analyser (EA-IRMS)

For analyses by flash combustion, an EA Isolink (Thermo Fisher) coupled to a continuous-flow isotope-ratio mass spectrometer (MAT253) via a Conflo VI (Thermo Finnigan) in the St Andrews Stable Isotope Geochemistry (STAiG) laboratory was used, following established methods (Kipp *et al.* 2019, Stüeken *et al.* 2020). Between 0.6–140 mg of sample was weighed into 9 × 5 mm tin capsules (Thermo Fisher). Samples were flash combusted with a stream of O_2 gas (250 ml min^{-1} for 5 s) in a column filled with granular chromium oxide and granular silvered cobaltous cobaltic oxide set to 1020 °C. The reagents were separated by 2 cm of quartz wool. The combustion column was followed by a reduction column packed with elemental copper wire at 600 °C to ensure complete conversion of nitrogen oxides to N_2 gas. Water was trapped with granular magnesium perchlorate at room temperature. To further optimise this method for silicate samples, we experimented with longer O_2 pulses, the O_2 flow rate, the temperature of the combustion and the addition of V_2O_5 powder as an additional combustion aid (see below).

Results and discussion

Calibration

For the calibration of nitrogen abundance and for converting measured isotopic ratios to the conventional delta notation, the international RM USGS-61 and USGS-62 (both caffeine) were used. These both have a published N mass fraction of 28.87% *m/m* and isotopic values of -2.87 ± 0.04‰ (USGS-61) and +20.17 ± 0.06‰ (USGS-62), respectively (Coplen 2019). It is noted that these calibrators have a different matrix than silicates; however, caffeine is relatively easy to combust, and as a pure chemical compound it contains a stoichiometrically set N mass fraction. Due to the dearth of existing silicate N RM, we must rely on well-established alternatives. The calibration curves for USGS-61 and USGS-62 are shown in Figure 2.

Analytical blanks

The blank that was applied to correct our data is the sum of all blank contributions (vacuum line + gas-line + reagents). This mean blank was determined from a compilation of all blanks measured on the sealed tube combustion line up to December 2019, monitored during each analytical session (Figure 3). Previous users of the sealed tube combustion method have variably used silver (Ag) capsules, CuO and Cu wire and CaO powder (Kendall and Grim 1990, Busigny *et al.* 2005, Bebout *et al.* 2007). The Ag capsules can be used as sample holders to easily transfer powdered material to the base of a 30-cm tube. Furthermore, Ag may act as a trap for sulfur gases liberated from the sample. The CaO is used to adsorb produced H_2O/CO_2. However, neither Ag nor CaO was used in this study. Instead, liquid nitrogen U-traps and a gas chromatograph column in the set-up (Figure 2) were used to purify the produced gases of molecules such as H_2O, CO, CO_2 and sulfur gases, resulting in a reduction in the total analytical blank size by > 50% (see below). No memory effects were observed in the tube cracker line operating under current conditions, tested by measuring the tube cracker line blank (see below) with no sample in the line.

To assess the necessity of different reagents in the analytical set-up, a number of blank combinations were tested (Ag + CuO + Cu, CuO + Cu and CuO only) and their respective impact on the total blank quantified. The mean CuO blank was 15.4 ± 3.8 nmol N (1*s*) with a mean $\delta^{15}N$ value of -1.73 ± 0.88‰ (1*s*, n = 20). The mean blank for CuO + Cu, used for SGR-1, was 24.0 ± 5.7 nmol N (1*s*) with a mean $\delta^{15}N$ value of -0.21 ± 1.92‰ (1*s*, n = 10). When silver capsules were used in combination with CuO (CuO + Ag), the blank increased to 19.7 ± 3.4 nmol N (1*s*) with a mean $\delta^{15}N$ value of -8.9 ± 0.9‰ (1*s*, n = 7). All three reagents combined (CuO + Cu + Ag) resulted in a blank of 52.1 ± 4.2 nmol N (1*s*) with a mean $\delta^{15}N$ value of -0.2 ± 2.5‰ (1*s*, n = 6). The vacuum line blank was assessed by measuring an empty, but evacuated tube that had undergone the same treatment as a normal

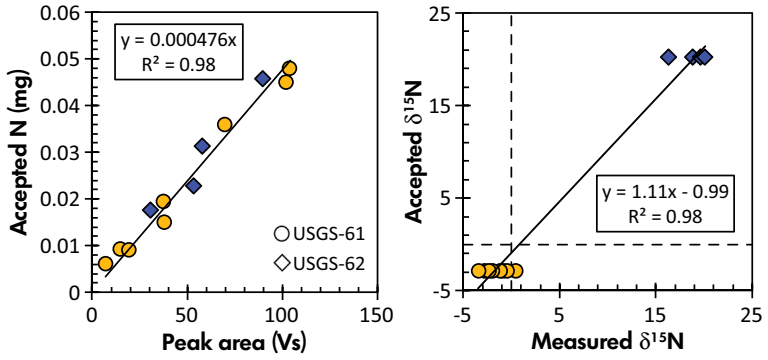

Figure 2. Calibration curves for N content and isotopes used to process the sealed tube data in this study. Errors on N mass fraction and isotope ratio are smaller than the symbols. Accepted values for USGS61 and USGS62 from Coplen (2019). [Colour figure can be viewed at wileyonlinelibrary.com]

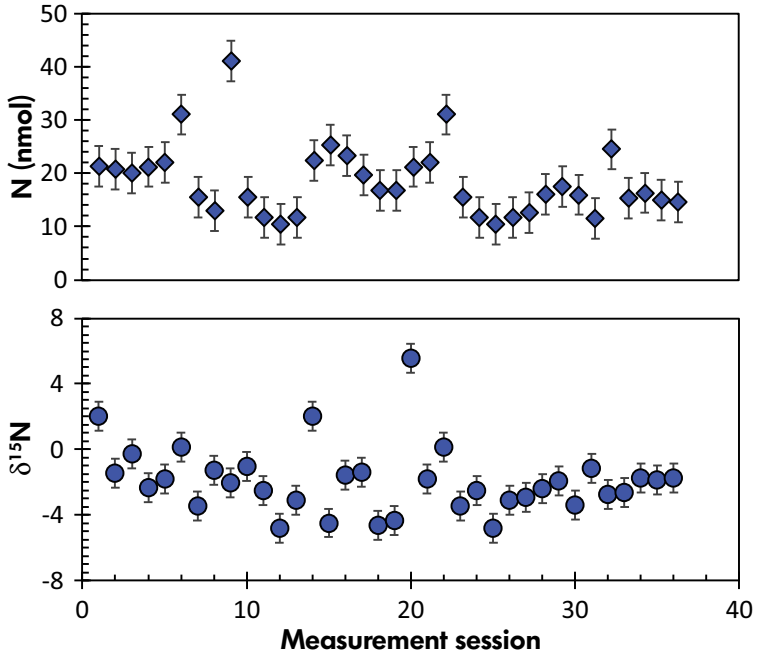

Figure 3. Analytical blanks (CuO only) through time over the course of roughly one year, showing N content and isotopes. The blanks remained relatively steady allowing for accurate blank corrections to be carried out on samples with low N content. Vertical range bars represent 1*s* of the mean. [Colour figure can be viewed at wileyonlinelibrary.com]

sample and resulted in a blank of 4.7 ± 2.6 nmol N (1*s*) with a mean δ^{15}N value of -7.6 ± 4.8‰ (1*s*, *n* = 14). The tube cracker line can also add to the blank if there are small leaks. This line blank was 0.7 ± 0.9 nmol N (1*s*) with a mean δ^{15}N value of -7.2 ± 9.5‰ (1*s*, *n* = 8). Therefore, the major contributor of the overall blank of 15.4 ± 3.8 nmol N (CuO only) was the CuO itself, followed by the blank associated with the vacuum line. This is attributed to trace impurities of the CuO that could not be removed by pre-treatment in the muffle furnace (see Materials section).

As noted above, the use of Ag capsules was avoided by inserting the sample powder with a thistle funnel or with hand-made quartz capsules, to ensure that the sample reached the base of the tube and was retained after blowtorch removal from the vacuum line. The addition of Cu was found to be unnecessary for most materials except for the SGR-1b oil shale. As a result, the CuO blank was used to correct for blank contributions in all samples except SGR-1b (which required Cu also, e.g., CuO + Cu blank correction). Figure 3 shows the evolution of the CuO blank over the

course of approximately 1 year, indicating relative stability and reproducibility. For data correction, the mean of these blank measurements was applied.

For the EA, the blank, resulting from the tin capsule and trace N_2 contained in the O_2 and He gases, was below detection with a 50 ml min^{-1} carrier flow rate. However, mass-balance calculations with a series of USGS-41 RM of different masses suggested the long-term EA blank to be roughly 11.2 ± 0.6 nmol (1*s*) N with an assumed isotopic value of approximately 0‰, representing minor leaks of air into the system.

Sealed tube method validation

To assess the accuracy of the new sealed tube combustion set-up at St Andrews, the IPGP in-house reference material MS#5 and the commercially available BHVO-2, for which there are published data using a sealed tube combustion method (Busigny *et al.* 2005, Feng *et al.* 2018), were used.

The measured mass fraction and $\delta^{15}N$ values for MS#5 and BHVO-2 in this study (Table 2) agree well with existing data (Busigny *et al.* 2005, Johnson *et al.* 2017, Feng *et al.* 2018). Differences for the blank-corrected nitrogen abundance and isotopic value were indistinguishable within uncertainty. However, it is worth noting that we obtained a slightly higher N abundance for MS#5 than Busigny *et al.* (2005) and Feng *et al.* (2018) but lower than that found by Boyd and Philippot (1998). This difference may be a result of slight differences in pre-combustion methods. For instance, Busigny *et al.* (2005) pre-combust at 500 °C compared with the 120 °C used in this study. They chose this higher temperature to ensure that all labile organic nitrogen was removed before sealed tube combustion, leaving only lattice-bound nitrogen to be liberated for analysis. However, there is a risk that some silicate-bound N is released at lower temperatures. Therefore, our pre-combustion temperature is conservative to make certain that no lattice-bound N is released. Alternatively, this difference could be a result of sample heterogeneity, as suggested by Boyd and Philippot (1998) but not indicated by Busigny *et al.* (2005) or Feng *et al.* (2018). Regardless of the difference in absolute N content, the different treatments had no significant impact on the measured isotope value.

Regarding BHVO-2, the nitrogen abundance data agreed well with Feng *et al.* (2018); however, the isotope value was approximately 1.1‰ lighter (though overlapping within 2*s* uncertainty). This small but consistent offset could indicate inter-sample heterogeneity as has been observed in a number of other isotope systems (e.g., Brett *et al.* 2018). Further analyses of this material at other laboratories should help determine whether BHVO-2 is a homogenous RM for nitrogen.

As a further test, existing reference material USGS-41 was used as quality control for the caffeine (USGS-61 and USGS-62) RM calibration curves. USGS-41 is an L-glutamic acid ($C_5H_9NO_4$) with 9.52% nitrogen and an isotope value of + 47.57‰ (Coplen *et al. 2011*, Jochum *et al.* 2005). As a pure isotope standard, this material has a stoichiometrically set N mass fraction and therefore is a good test to make sure that the sealed tube combustion method does not overestimate N mass fractions. Using the sealed tube combustion method, this study obtained a nitrogen mass fraction of 9.56 ± 0.06% (1s, $n = 3$) and an isotope value of + 47.22 ± 0.64‰ (1s, $n = 3$), which matches closely within uncertainty the published values for this reference material. This agreement indicates that the sealed tube method does not overestimate N mass fractions and therefore suggests that the values obtained for silicates using the sealed tube combustion method are accurately calibrated.

In summary, the nitrogen mass fractions and isotopic values that were measured with the sealed tube method for two mineralogically distinct silicate RMs (mica schist, basalt) and for a synthetic organic compound (L-Glutamic Acid) are in good agreement with published data, demonstrating that this method is suitable for the analysis of a wide range of materials.

Table 2.
A compilation of existing N reference materials with published values obtained using the sealed tube method

	N (µg g^{-1})	1*s*	$\delta^{15}N$ [‰]	1*s*
BHVO-2				
This study	23.4	1.8	+1.8	0.4
Feng *et al.* (2018)	26.6	2.3	+2.9	0.5
MS#5				
This study	294.3	10.8	+15.0	0.2
Boyd and Philippot (1998)	323.0		+14.8	
Busigny *et al.* (2005)	244.9	11.2	+14.9	0.5
Feng *et al.* (2018)	245.6	11	+14.35	0.1

1*s* = standard deviation.

Elemental analyser versus sealed tube combustion

Thirteen geological RM and one in-house reference material were analysed for N mass fraction and isotope values using both the EA and sealed tube combustion methods (Table 3). All materials were measured more than three times with each method to determine the degree of intra-sample heterogeneity. For the EA method, relative errors (1*s*/mean value) in the N mass fractions were between ± 2.5% and ± 26.6%, and for isotope values, the uncertainties (1*s*) were between ± 0.3‰ and ± 3.8‰. For the sealed tube combustion method, errors in the N mass fractions were between ± 3.7% and ± 19.8% with errors in the isotope values between ± 0.1‰ and ± 3.1‰. The nitrogen yield (calculated as sealed tube – EA abundances) was consistently lower for the EA, suggesting that the EA liberates between 33 and 69% of nitrogen compared with the sealed tube method, consistent with previous studies (Bräuer and Hahne 2005, Ader *et al.* 2006, Johnson *et al.* 2017, Feng *et al.* 2018).

Improving the yield of the EA method would be preferable over using sealed tube combustion, as the EA method is automated, cheaper and allows for a greater number of samples to be run per day. A number of tests were therefore formulated within the feasible operating parameters of the EA aimed at improving combustion of silicate materials. These were as follows: (a) multiple consecutive combustions of the same sample; (b) increasing the temperature that the furnace is held at pre-combustion; (c) varying the magnitude, timing and duration of the O_2 pulse; and (d) adding V_2O_5 powder to act as a combustion aid. None of these tests improved the EA yield to more than a mean of 69% (Test 4 – Table 4). Yields could also not be improved with multiple consecutive combustion steps (Figure 4a), counter to what has previously been achieved for the combustion of diamond (Mikhail *et al.* 2019). In addition, modifications to the EA method [greater O_2 flow rate, higher temperature (Figure 4b) or addition of V_2O_5 (Figure 4c)] did not produce a satisfactory increase in nitrogen yield. In short, changes to the EA parameters within the explored operational bounds failed to fully liberate lattice-bound N from silicates. Han *et al.* (2017) found that increasing the amount of O_2 during combustion in the EA did improve N yield in SGR-1b, obtaining a mass fraction of 0.91% *m/m* in comparison with the 1.16% *m/m* measured by the sealed tube method in this study. This offers promise to suggest the EA method may be improved with further work.

The mean relative error on N mass fractions for all measured RMs (Table 3) was 9.3% with the EA and 11.6% with the sealed tube method, showing that the sealed tube combustion method had comparable errors to the automated EA. Generally, the EA produced better yields for mafic rocks [e.g., BHVO-2 (47%), trachyte ISH-G (53%) and trachyte MDO-G (52%)] compared with felsic rocks [Granite MA-N (39%)]. This trend could be a result of differences in mineral grain size, as the felsic RMs are more coarsely crystalline, and therefore harder to combust. The isotopic value determined with the EA differed from the sealed tube value by -1.4‰ on average (Table 3). This offset is likely a kinetic fractionation resulting from low total yields for the EA method. For some materials, both methods produced isotope values identical within 1*s* uncertainty (BHVO-2, Trachyte MDO-G, Granite MAN and Shale SGR-1b), but there are few similarities between these RM in terms of lattice structures, mineralogy, mineral size, or temperature and environment of formation. Therefore, it is recommended that EA is not be used for analysing silicate materials when measuring nitrogen hosted in these mineral lattices.

Silicate nitrogen reference materials

Research on nitrogen cycling in silicate systems is expanding, and thus, it is essential to have well-characterised, homogeneous, commercially available and matrix-matched RM for data quality control both within and between laboratories. Hence, a large part of this study is aimed at addressing a dearth in existing silicate nitrogen RM that are representative of rocks typical within the Earth system (i.e., silicate phases).

Eleven commercially available RM were chosen to span a range of matrix types, both mineral and bulk rock. These include mafic rocks [basalt, trachyte (×2)], minerals (biotite, phlogopite, serpentine), felsic rocks [granite (×2)], minerals (albite, anorthite, K-feldspar), sedimentary (shale) and metamorphic [mica schist (×2)] rocks. This study presents the first data recorded for N mass fractions and isotope values for eleven of these materials. Using the sealed tube combustion method, the silicate RM ranged from < 10 μg g^{-1} to 1% *m/m* nitrogen mass fractions and $\delta^{15}N$ of -0.5 to + 19.8‰ (Figure 5) which broadly represents values consistent with the Earth's continental crust (Johnson and Goldblatt 2015).

A good RM must show homogeneity of the element of interest. Full repeat analysis is a straightforward way to assess whether a RM is sufficiently homogenous within the bounds of current measurement precision. This is particularly important in element systems that are susceptible to bimodal distribution of the element of interest. In the case of N, such bimodality is highly likely. For instance, in a simple quartz–-feldspar–mica system the nitrogen mass fraction of quartz

Table 3.
Measured values for all reference materials using the EA and sealed tube methods

Sample ID	Elemental analyser						Sealed tube combustion						EA yield (%)	$\Delta^{15}N_{EA-TC}$ (‰)
	n	N (μg g^{-1})	1*s*	% error	$\delta^{15}N$ (‰)	1*s*	*n*	N (μg g^{-1})	1*s*	% error	$\delta^{15}N$ (‰)	1*s*		
Albite ALI	4	5.6	1.5	27	+3.3	1.8	5	14.0	2.4	17	+4.0	0.1	40	-0.69
Anorthosite ANG	4	4.5	1.2	26	+0.2	3.0	5	13.2	1.7	13	+4.7	0.3	34	-4.52
BHVO-2	6	10.9	0.3	3	+1.3	0.9	6	23.4	1.8	8	+1.8	0.4	47	-0.53
Felspath FKN	7	3.7	0.2	7	-1.5	2.3	6	10.9	1.0	9	+4.5	0.6	34	-5.97
Serpentinite UB-N	4	11.9	0.4	3	+0.8	1.8	4	27.5	1.6	6	+4.0	0.3	43	-3.18
Trachyte ISH-G	4	17.7	1.0	5	+15.1	1.0	4	33.2	5.1	15	+19.8	3.1	53	-4.70
Trachyte MDO-G	4	5.9	0.9	16	-0.7	3.8	4	11.3	1.4	12	-0.5	0.5	52	-0.18
Biotite Fe	10	104.6	9.9	9	+8.3	1.0	9	245.1	23.0	9	+7.5	0.3	43	+0.73
Granite MAN	5	50.4	1.7	3	+5.7	0.4	7	128.2	10.3	8	+6.0	0.7	39	-0.30
Phlogopite Mg	4	7.7	0.6	8	+12.0	1.8	5	16.8	3.3	20	+5.6	0.7	46	+6.45
Mica Schist SDC-1	3	4.8	0.1	3	+3.9	2.0	5	14.4	2.8	19	+7.7	1.0	33	-3.77
Shale SGR-1b	5	7945	196	2	+18.1	0.3	5	11584	431	4	+18.0	0.7	69	+0.16
Granite G3	–	–	–	–	–	–	6	22.8	2.7	12	+3.2	1.0	–	–

By comparison, the EA failed to obtain the same values for N contents or isotopes. The sealed tube method tends to have comparable % errors on N contents with generally smaller standard deviation (1*s*) for isotope values.
n = number of replicate analyses of a separate powder aliquot.

GEOSTANDARDS and GEOANALYTICAL RESEARCH

Table 4.
Results of comprehensive EA-IRMS parameter testing

Sample	Sealed tube RM		EA RM		Yield (%)	Test 1		Yield (%)	Test 2		Yield (%)	Test 4		Yield (%)	Test 5		Yield (%)
	N (µg g^{-1})	δ^{15}N (‰)	N (µg g^{-1})	δ^{15}N (‰)		N (µg g^{-1})	δ^{15}N (‰)		N (µg g^{-1})	δ^{15}N (‰)		N (µg g^{-1})	δ^{15}N (‰)		N (µg g^{-1})	δ^{15}N (‰)	
BHVO-2	23.4	+1.8	10.9	+1.3	47	8.1	+1.2	35	13	+2.5	56	15.9	+1.1	68	12.6	-1.7	54
Biotite-Fe	245.1	+7.5	105	+9.9	43	106	+4.8	43	93	+5.3	38	133	+3.8	54	94	+4.4	38
Felspath FK-N	10.9	+4.5	3.7	-1.5	34	4.0	+4.1	37	6.0	+1.7	55	9.7	+5.6	89	6.0	-4.8	55
Granite MA-N	128.2	+6.0	50	+5.7	39	53	+3.1	41	63	+6.1	49	84	+5.3	65	63	+2.9	49
Method																	
Temperature (°C)			1020			1100			1020			1020			1020		
Sampling delay (s)			20			20			20			12			10		
O_2 pulse duration (s)			5			5			8			8			10		

Four reference materials that span mafic and felsic rocks and minerals were chosen for this testing. The effect of increasing temperature, and oxygen quantity and timing were found to have insufficient effect on improving the nitrogen yield. The longer the sampling delay, the shorter the time that the sample is heated prior to the arrival of the O2 pulse. The O2 pulse was always injected at a flow rate of 250 ml min-1 at 2.5 bar pressure. He pressure was 2.5 bar at a constant flow rate of 50 ml min^{-1}.

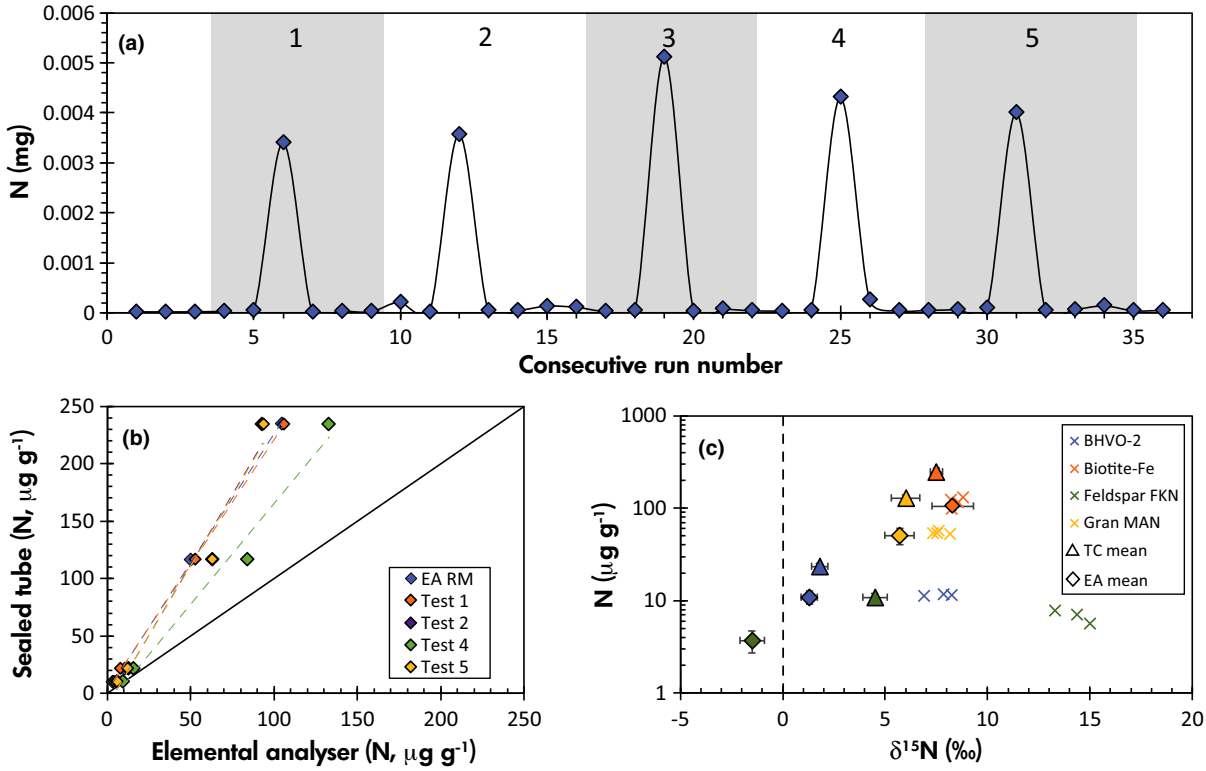

Figure 4. (a) Test using Biotite-Fe reference material to determine whether repeat EA combustions improve silicate N liberation under standard conditions. The first four values establish the background blanks with no capsules (e.g., background blank of the EA). Peaks represent combustion of biotite, followed by four blanks, allowing potential sample residues to undergo four additional combustions. There is no evidence that repeat combustions improve the EA yield. (b) Comparison of different test parameters (see Table 4) aimed at improving EA yields. In every case, the EA fails to reproduce the values obtained through sealed tube combustion. (c) Test using V_2O_5 powder as a combustion aid for liberating silicate-bound N on the EA. Crosses show results of analyses of four different silicate reference materials spanning a range in matrix types. In all cases, a sample:V_2O_5 ratio of 10:1 was used. Filled diamonds are the mean result obtained from the EA under standard operating conditions without V_2O_5. Filled triangles are mean values obtained from the sealed tube combustion without V_2O_5. Note that in every case, the addition of V_2O_5 powder results in isotopically heavier values with little improvement to overall N yield. The addition of V_2O_5 as a combustion aid does not result in an accurate or precise nitrogen data relative to the sealed tube combustion method. [Colour figure can be viewed at wileyonlinelibrary.com]

compared with feldspar or mica would be negligible (see discussion of Boyd *et al.* 1993), because reduced nitrogen species (NH_4^+) preferentially substitute for alkali metals such as K^+ or Rb^+ (Li *et al.* 2013) due to similar ionic charge and radius. As a result, mica tends to contain larger N mass fractions than feldspar (Hall 1999). However, mica is typically volumetrically much less significant in granitic rocks compared with feldspar. Such concerns are not restricted to felsic plutonic rocks. For example, BHVO-2 has previously been found to be heterogeneous for lead (Pb; Chauvel *et al.* 2011), lithium (Li; Li *et al.* 2019) and thallium (Tl; Brett *et al.* 2018), which has been attributed to mineralogically controlled bimodal distributions of these elements. In the case of N mass fractions, BHVO-2 is homogenous according to our repeat analyses within the bounds of our analytical precision; however, it is worth recalling that we failed to obtain the same isotope value as Feng *et al.* (2018), which could indicate intra-sample heterogeneity. Further work with this RM is recommended to determine N hetero/homogeneity.

The most homogenous RMs according to our data for N mass fractions and isotope values are BHVO-2, Serpentine UB-N, Felspath FK-N and Biotite-Fe. The most heterogeneous RMs are Mica Schist SDC-1 and Trachyte ISH-G, perhaps due to large inter-mineral bimodality for N (e.g., mica and orthoclase dominate the assemblages, respectively).

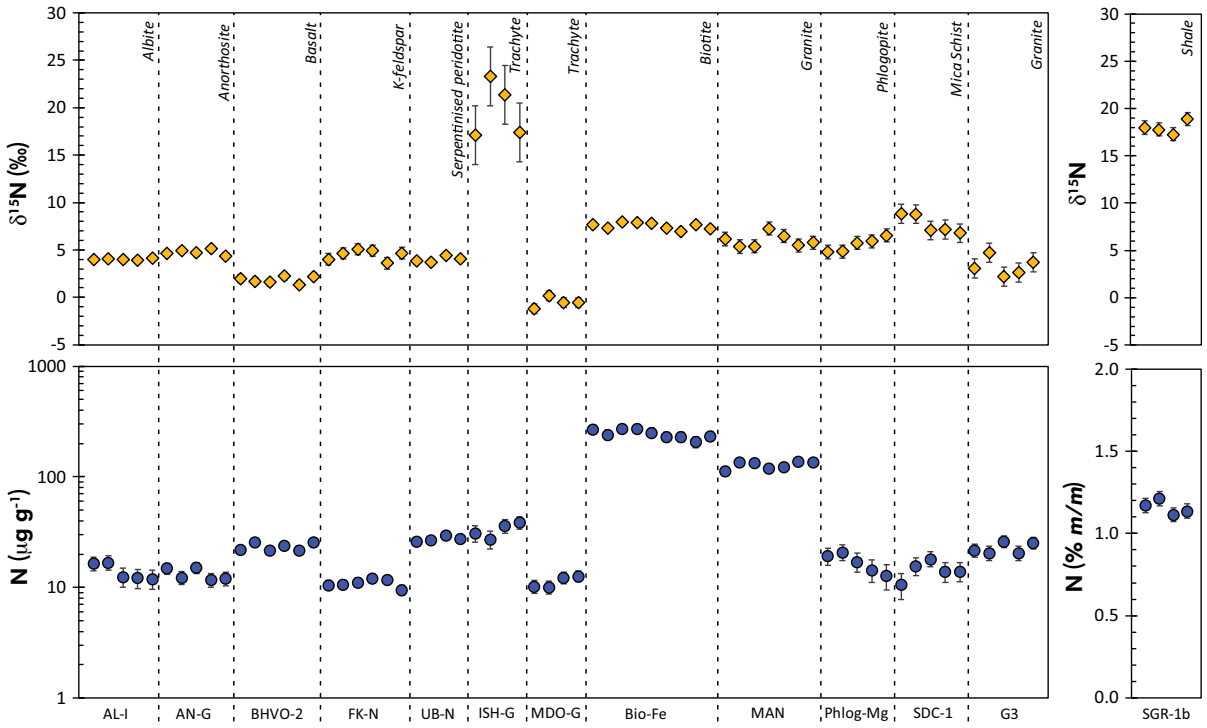

Figure 5. Comparison of all sealed tube nitrogen data for geological reference materials measured in this study (see Table 1). All range bars shown represent 1*s* on the mean of replicate analyses with many being smaller than the symbols. [Colour figure can be viewed at wileyonlinelibrary.com]

Conclusions

Data quality for the sealed tube method

The new sealed tube facility can accurately and precisely quantify the nitrogen abundance and isotopic value for nanomole quantities of N_2 gas liberated from silicate matrices. Given the current blank [15.4 ± 3.8 nmol N, $\delta^{15}N$ -1.73 ± 0.88‰ (1*s*, *n* = 20)], a sample with *ca.* 10 μg g^{-1} N requires around 200–300 mg of sample to obtain a signal/blank ratio better than 10:1, which is appropriate for a wide range of geological applications. The gasline has been optimised to require only short inter-sample purging times, reduced from 45 min to < 3 min, allowing for a relatively high sample throughput of 16–20 tubes per day (including samples, RM and blanks). Inter-laboratory comparison of the new sealed tube combustion method at St Andrews with those of Université de Paris (MS# 5: Busigny *et al.* 2005) and the Chinese Academy of Science (BHVO-2: Feng *et al.* 2018) replicates previously published values within the bounds of current analytical precision.

Limitations of the EA for silicate materials

The EA method is unsuitable for the quantification of nitrogen mass fractions and isotopic values for silicate samples where nitrogen is lattice-bound. Inaccuracies in the EA method have previously been highlighted for Precambrian sedimentary rocks and for BHVO-2 (Bräuer and Hahne 2005, Ader *et al.* 2006, Johnson *et al.* 2017, Feng *et al.* 2018). The data of this study suggest the EA method routinely underestimates the nitrogen mass fraction by > 50%, which also results in kinetic isotope fractionation associated with incomplete liberation of nitrogen from the silicate lattice. This effect was observed in all materials (except for the synthetic organic USGS RM), regardless of differences in organic content, matrix type, geological source or crystallinity of the materials. Full liberation of lattice-bound nitrogen in silicate materials requires diffusion at high temperatures. The incomplete liberation of N using the EA method is attributed to differences between the flash heating (5 s) set-up of an EA compared with the longer heating times (6 h) of sealed tubes, because the release of nitrogen is a diffusive process. Improvements to nitrogen yields using the EA method were not possible within reasonable bounds of EA operating conditions. The EA has many operational benefits (cheaper, automated, higher sample throughput) compared with the sealed tube combustion method and therefore would be preferable if modifications to the method can be made to improve accuracy. It is worth stressing that the EA remains an excellent tool for many materials (e.g.,

organics) but care should be taken when analysing silicate materials and interpreting both N mass fractions and $\delta^{15}N$ from silicates using the EA method.

Identification of silicate reference materials

Nitrogen mass fraction and isotope ratio values were reported for fourteen silicate RM chosen to span the range of crustal signatures. The first reported N mass fraction and isotope values for eleven geochemical RM, Albite AL-I, Anorthosite AN-G, Felspath FK-N, Serpentine UB-N, Trachyte ISH-G, Trachyte MDO-G, Biotite-Fe, Phlogopite-Mg, Granite MA-N, Mica Schist SDC-1 and Granite G3 have been determined. Of these, BHVO-2, Serpentine UB-N, Felspath FK-N and Biotite-Fe are the most appropriate for use as reference materials for nitrogen in the future.

Acknowledgements

Financial support was provided by a NERC IAPETUS Doctoral Training Programme (NE/R012253/1) studentship (TJB) and by the School of Earth and Environmental Sciences at St Andrews (EES). SM acknowledges support from NERC standard grant NE/PO12167/1. We thank Vincent Busigny (IPGP) for sharing in-house reference material (MS#5) and Stephen Wilson (USGS) for providing RM G3. The handling editor and one anonymous reviewer are thanked for constructive feedback that improved the manuscript.

Conflict of interest

The authors declare no conflict of interests.

Data Availability Statement

The data that support the findings of this study are available in the supplementary material of this article.

References

Ader M., Cartigny P., Boudou J.-P., Oh J.-H., Petit E. and Javoy M. (2006)
Nitrogen isotopic evolution of carbonaceous matter during metamorphism: Methodology and preliminary results. **Chemical Geology, 232**, 152–169.

Barry P.H., Hilton D.R., Halldórsson S.A., Hahm D. and Marti K. (2012)
High precision nitrogen isotope measurements in oceanic basalts using a static triple collection noble gas mass spectrometer. **Geosystems Geochemistry Geophysics, 13**, 1–16.

Bebout G.E. and Fogel M.L. (1992)
Nitrogen-isotope compositions of metasedimentary rocks in the Catalina Schist, California: Implications for metamorphic devolatilization history. **Geochimica et Cosmochimica Acta, 56**, 2839–2849.

Bebout G.E. and Sadofsky S.J. (2004)
$\delta^{15}N$ analyses of ammonium-rich silicate minerals by sealed-tube extractions and dual inlet, viscous-flow mass spectrometry. **In: de Groot, P.A. (ed.), Handbook of stable isotope analytical techniques**, Volume 1. **Elsevier Science (Amsterdam)**, 348–360.

Bebout G.E., Idleman B.D., Li L. and Hilkert A. (2007)
Isotope-ratio-monitoring gas chromatography methods for high-precision isotopic analysis of nanomole quantities of silicate nitrogen. **Chemical Geology, 240**, 1–10.

Boyd S.R. and Pillinger C.T. (1990)
Determination of the abundance and isotope composition of nitrogen within organic compounds: A sealed tube technique for use with static vacuum mass spectrometers. **Measurement Science Technology, 1**, 1176–1183.

Boyd S.R., Hall A. and Pillinger C.T. (1993)
The measurement of $\delta^{15}N$ in crustal rocks by static vacuum mass spectrometry: Application to the origin of the ammonium in the Cornubian batholith, southwest England. **Geochimica et Cosmochimica Acta, 57**, 1339–1347.

Boyd S.R., Rejou-Michel A. and Javoy M. (1994)
Noncryogenic purification of nanomole quantities of nitrogen gas for isotopic analysis. **Analytical Chemistry, 66**, 1396–1402.

Boyd S.R. and Philippot P. (1998)
Precambrian ammonium biogeochemistry: A study of the Moine metasediments, Scotland. **Chemical Geology, 144**, 257–268.

Bräuer K. and Hahne K. (2005)
Methodical aspects of the ^{15}N-analysis of Precambrian and Palaeozoic sediments rich in organic matter. **Chemical Geology, 218**, 361–368.

Brett A., Prytulak J., Hammond S.J. and Rehkämper M. (2018)
Thallium mass fraction and stable isotope ratios of sixteen geological reference materials. **Geostandards and Geoanalytical Research, 42**, 339–360.

Busigny V., Ader M. and Cartigny P. (2005)
Quantification and isotopic analysis of nitrogen in rocks at the ppm level using sealed tube combustion technique: A prelude to the study of altered oceanic crust. **Chemical Geology, 223**, 249–258.

Busigny V. and Bebout G.E. (2013)
Nitrogen in the silicate Earth: Speciation and isotopic behaviour during mineral-fluid interactions. **Elements, 9**, 353–358.

references

Chauvel C., Bureau S. and Poggi C. (2011)
Comprehensive chemical and isotopic analyses of basalt and sediment reference materials. **Geostandards and Geoanalytical Research**, **35**, 125–143.

Coplen T. (2011)
Reston stable isotope laboratory report of stable isotopic composition: Reference material USGS41. **United States Geological Survey.**

Coplen T. (2019)
Reston stable isotope laboratory report of stable isotopic composition: Reference materials USGS61, USGS62 and USGS63. **United States Geological Survey.**

Craig H. (1953)
The geochemistry of stable carbon isotopes. **Geochimica et Cosmochimica Acta**, **3**, 53–92.

Dennen K.O., Johnson C.A., Otter M.L., Silva S.R. and Wandless G.A. (2006)
$\delta^{15}N$ and non-carbonate $\delta^{13}C$ values for two petroleum source rock reference materials and a marine sediment reference material. **US Geological Survey Open-File Report.**

Feng L., Li H. and Liu W. (2018)
Nitrogen mass fraction and isotope determinations in geological reference materials using sealed-tube combustion coupled with continuous-flow isotope-ratio mass spectrometry. **Geostandards and Geoanalytical Research**, **42**, 539–548.

Goldschmidt V. (1926)
Geochemical distribution law of the elements. VII. Summary of the chemistry of crystals. **Naturwissenschaften**, **14**, 477–485.

Hall A. (1999)
Ammonium in granites and its petrogenetic significance. **Earth-Science Reviews**, **45**, 145–165.

Han W., Feng L., Li H. and Liu W. (2017)
Bulk $\delta^{15}N$ measurements of organic-rich rock samples by elemental analyzer/isotope ratio mass spectrometry with enhanced oxidation ability: Bulk $\delta^{15}N$ measurements of organic-rich rock samples. **Rapid Communications in Mass Spectrometry**, **31**, 16–20.

Jochum K.P., Nohl U., Herwig K., Lammel E., Stoll B. and Hofmann A.W. (2005)
GeoReM: A new geochemical database for reference materials and isotopic standards. **Geostandards and Geoanalytical Research**, **29**, 333–338.

Johnson B. and Goldblatt C. (2015)
The nitrogen budget of Earth. **Earth-Science Reviews**, **148**, 150–173.

Johnson B.W., Drage N., Spence J., Hanson N., El-Sabaawi R. and Goldblatt C. (2017)
Measurement of geologic nitrogen using mass spectrometry, colorimetry, and a newly adapted fluorometry technique. **Solid Earth**, **8**, 307–318.

Kendall C. and Grim E. (1990)
Combustion tube method for measurement of nitrogen isotope ratios using calcium oxide for total removal of carbon dioxide and water. **Analytical Chemistry**, **62**, 526–529.

Kipp M.A., Stüeken E.E., Gehringer M.M., Sterelny K., Scott J.K., Forster P.I., Strömberg C.A.E. and Buick R. (2019)
Exploring cycad foliage as an archive of the isotopic composition of atmospheric nitrogen. **Geobiology**, 1–15.

Kubota R. (2009)
Simultaneous determination of total carbon, nitrogen, hydrogen and sulfur in twenty-seven geological reference materials by elemental analyser. **Geostandards and Geoanalytical Research**, **33**, 271–283.

Li Y., Wiedenbeck M., Shcheka S. and Keppler H. (2013)
Nitrogen solubility in upper mantle minerals. **Earth and Planetary Science Letters**, **377–378**, 311–323.

Li W., Liu X.-M. and Godfrey L.V. (2019)
Optimisation of lithium chromatography for isotopic analysis in geological reference materials by MC-ICP-MS. **Geostandards and Geoanalytical Research**, **43**, 261–276.

Marty B., Lenoble M. and Vassard N. (1995)
Nitrogen, helium and argon in basalt: A static mass spectrometry study. **Chemical Geology**, **120**, 183–195.

Mikhail S. and Sverjensky D.A. (2014)
Nitrogen speciation in upper mantle fluids and the origin of Earth's nitrogen-rich atmosphere. **Nature Geoscience**, **7**, 816–819.

Mikhail S., Howell D., Hutchison M., Verchovsky A.B., Warburton P., Southworth R., Thompson A.R., Jones A.P. and Mileage H.J. (2014)
Constraining the internal variability of carbon and nitrogen isotopes in diamonds. **Chemical Geology**, **366**, 14–23.

Mikhail S., McCubbin F.M., Jenner F.E., Shirey S.B., Rumble D. and Bowden R. (2019)
Diamondites: Evidence for a distinct tectono-thermal diamond-forming event beneath the Kaapvaal craton. **Contributions to Mineralogy and Petrology**, **174**, 71.

Minagawa M. and Wada E. (1986)
Nitrogen isotope ratios of red tide organisms in the East China Sea: A characterization of biological nitrogen fixation. **Marine Chemistry**, **19**, 245–259.

Stüeken E.E., Buick R., Guy B.M. and Koehler M.C. (2015)
Isotopic evidence for biological nitrogen fixation by molybdenum-nitrogenase from 3.2 Gyr. **Nature**, **520**, 666–669.

Stüeken E.E., Tino C., Arp G., Jung D. and Lyons T.W. (2020)
Nitrogen isotope ratios trace high pH conditions in a terrestrial Mars analogue site. **Science Advances**, **6**, 1–8.

references

Stuermer D.H., Peters K.E. and Kaplan I.R. (1978)
Source indicators of humic substances and proto-kerogen. Stable isotope ratios, elemental compositions and electron spin resonance spectra. **Geochimica et Cosmochimica Acta, 42**, 989–997.

Urey H.C. (1947)
The thermodynamic properties of isotopic substances. **Journal of the Chemical Society**, 562–581.

Wilson S.A. (1997)
Data compilation for USGS reference material BHVO-2, Hawaiian basalt. **US Geological Survey Open-File Report**.

Yoshioka T., Wiedenbeck M., Shcheka S. and Keppler H. (2018)
Nitrogen solubility in the deep mantle and the origin of Earth's primordial nitrogen budget. **Earth and Planetary Science Letters, 488**, 134–143.

Supporting information

The following supporting information may be found in the online version of this article:

Appendix S1. Elemental analyser and tube cracker measurement results; summary nitrogen data for reference materials; calibration data for USGS-61, USGS-62 and USGS41.

This material is available from: http://onlinelibrary.wiley.com/doi/10.1111/ggr.12345/abstract (This link will take you to the article abstract).